JOURNAL OF CATALYSIS 77, 180–191 (1982)

The Influence of Crystallographic Shear Planes on the Behavior of Molybdenum–Tungsten Oxide Catalysts for the Selective Oxidation of Propene

SARAH BARBER,*,[1] J. BOOTH,* D. R. PYKE,*,[2] R. REID,* AND R. J. D. TILLEY†

*I.C.I. Corporate Laboratory, P.O. Box 11, The Heath, Runcorn, Cheshire, England, and †School of Materials Science, University of Bradford, Bradford BD7 1DP, England

Received November 30, 1981; revised March 30, 1982

The selective oxidation of propene to propenal has been investigated for two series of molybdenum–tungsten oxide catalysts. The first series had the general formula $Mo_xW_{1-x}O_3$ and a WO_3-like structure, while members of the second series of general formula $(Mo_xW_{1-x})_nO_{3n-1}$ had crystallographic shear structures. Members of the latter series showed a higher conversion and selectivity than the corresponding members of the first series. Selectivity was found to decrease as the tungsten content increased and as the density of crystallographic shear planes decreased. *In situ* oxidation of the reduced series $(Mo_xW_{1-x})_nO_{3n-1}$ resulted in little change in selectivity but a significant fall in conversion.

INTRODUCTION

There has recently been much discussion about the role which crystallographic shear (*CS*) planes may play in the catalytic behavior of certain oxides. O'Keeffe has suggested that *CS* planes may greatly facilitate the transport of oxygen through the lattice (*1*). This would influence the rate of reoxidation of surface sites by lattice oxygen and thus be important in governing the catalytic behavior (*2*). In addition there has been speculation as to whether the shearing mechanism is also important in *selectively* making oxygen available to organic reactant during catalytic oxidation (*2, 3*). Metal oxide lattices *containing cations from groups IV, V, VI,* which are able to form *CS* structures, possess the ability to switch readily from a corner- to an edge-sharing or an edge- to face-sharing linkage of metal oxygen polyhedra, thus making an oxygen atom available for reaction. Active catalysts containing these cations, though not necessarily containing ordered *CS* planes (*4*), might by this mechanism insert oxygen into adsorbed hydrocarbon molecules to give selective oxidation products. Some experiments relevant to these ideas are contained in a series of studies by Schiavello *et al.* (*5–10*). These authors have studied a number of reduced tungsten oxides and have shown that catalysts containing *CS* planes were more selective than unreduced WO_3 for the oxidation of propene to propenal. The materials were, however, unstable under the reaction conditions, oxidizing rapidly and losing their catalytic activity.

In a similar vein, the *in situ* reduction of MoO_3 has been studied by Gai (*11*) within a reaction cell in a high voltage electron microscope. The dynamic formation of defects and *CS* planes has been investigated and the subsequent behavior in a propene/oxygen environment described. Parallel experiments in an external chemical reactor make this a potentially powerful technique for correlating catalytic performance with microstructure under reaction conditions.

The object of the work reported here was to explore these ideas in more detail by

---

[1] Present address: Churchill College, Cambridge CB3 ODS, England.

[2] To whom correspondence should be addressed.

0021-9517/82/090180-12$02.00/0

making rather more stable oxides containing *CS* planes and relating their structure closely to their catalytic behavior. To do this it would be desirable to study oxides containing just one metal cation, but as both the catalytic effectiveness and the stability of the system must be considered, we are more constrained in our selection of suitable materials. However, one group of *CS* oxides which is suitable both crystallographically and catalytically is to be found in the ternary Mo–W–O system and has the general formula $(Mo_xW_{1-x})_nO_{3n-1}$.

The crystal chemistry of both the binary and ternary molybdenum and tungsten oxides is fairly complex and has prompted the publication of a number of review articles in recent years (*12–15*). All the compounds we are concerned with have structures closely related to that of tungsten trioxide, WO_3, an idealized representation of which is shown in Fig. 1, where it can be seen that the building blocks for the material are WO_6 octahedra. These are linked together by corner sharing via oxygen atoms to form a three-dimensional chessboard-like array. In WO_3 itself the small cations are off-center in the octahedra, leading to small distortions of the structure which both lower the symmetry and increase the unit cell size. When MoO_3 is reacted with WO_3, to produce a series of fully oxidized phases $Mo_xW_{1-x}O_3$, the same WO_3 type of structure is retained over almost all of the composition range (*16*).

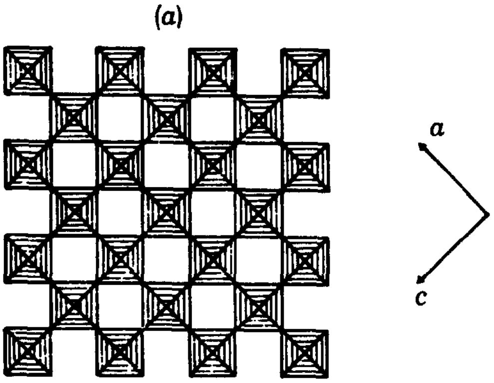

FIG. 1. Idealized representation of the crystal structure of WO_3. Shaded squares represent the three-dimensional array of corner-linked WO_6 octahedra. If the octahedra were not tilted the structure would be cubic and of the ReO_3 (DO_9) type.

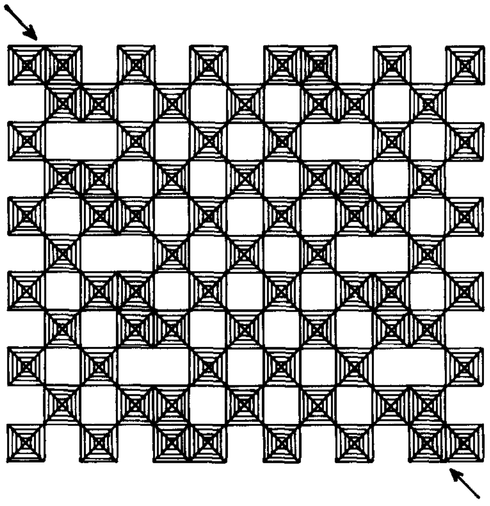

FIG. 2. The idealized structure of {102} *CS* planes, which are composed of blocks of four edge-shared octahedra and are separated by slabs of WO_3-like corner-sharing octahedra. The compound shown is $(Mo,W)_{11}O_{32}$. Other members of the $(Mo,W)_nO_{3n-1}$ series have either wider or narrower separation of the *CS* planes. The value of *n* in this formula is equal to the number of metal–oxygen octahedra between *CS* planes counted in the direction indicated by the arrows.

The phases which form when oxygen is lost from the fully oxidized $Mo_xW_{1-x}O_3$ phases depend both on the temperature of reduction and the degree of reduction (*17*). In this paper we have limited our study to the series of *CS* phases which lie along the composition lines between WO_3 and the binary molybdenum oxides Mo_8O_{23} and Mo_9O_{26}. The idealized structure of a typical member of this series is shown in Fig. 2 where it can be seen that much of the structure consists of the same WO_3-like array of corner-sharing metal–oxygen octahedra to be found in the fully oxidized phases. Prominent features in the structure, though, are the *CS* planes, which are defined by the blocks of four edge-sharing octahedra lying on {102} planes with respect to the idealized cubic unit cell of the WO_3-like part of the structure.

Within the series of *CS* phases that we are studying, one compound differs from another mainly in the number and distribution of the *CS* planes present in the crystals. If the *CS* planes are ordered the composition is given by the formula $(Mo, W)_nO_{3n-1}$, where *n* is the number of metal–oxygen octahedra separating the *CS* planes, as shown in Fig. 2. In the present system *n* takes integral values from 8 and 9 for the binary oxides Mo_8O_{23} and Mo_9O_{26} up to about 14, for $(Mo,W)_{14}O_{41}$.

In practice, the degree of ordering of the *CS* planes in real crystals is very variable, being greatest in those materials in which the *CS* plane spacing is smallest and the *CS* planes are most densely packed.

In the present study we have chosen the oxidation of propene as a test reaction to investigate the importance of *CS* planes in catalysis. For comparison, the series of unreduced molybdenum tungsten oxides of general formula $Mo_xW_{1-x}O_3$ which does not contain *CS* planes was also studied. This paper discusses the relationship between the catalytic behavior and the crystal chemistry of the starting materials and we attempt to assess the role of the *CS* planes in the chemical reactions which take place.

EXPERIMENTAL

a. Sample preparation. Oxides of formula $(Mo_xW_{1-x})_nO_{3n-1}$ were prepared by mixing appropriate amounts of WO_3 (BDH), MoO_3 (BDH AnalaR), and MoO_2 (K. & K. Laboratories Inc.). The mixtures were heated in evacuated sealed silica tubes in stages up to 700°C and held there for 3 weeks. After this time the furnace was turned off and the samples allowed to cool *in situ*. The series $Mo_xW_{1-x}O_3$ was prepared in a similar way. Mixtures of the appropriate amounts of WO_3 and MoO_3 were heated in evacuated, sealed silica tubes in stages up to 775°C. They were then held at 775°C for 11 days, the furnace turned off, and the samples allowed to cool *in situ*.

b. Sample characterization. The samples were characterized structurally both before and after catalysis using X-ray diffraction and transmission electron microscopy. Powder X-ray diffraction patterns of finely ground samples were obtained on either a Philips automatic powder diffractometer using CuKα radiation, or a Guinier–Hägg focusing camera using strictly monochromatic $CuK\alpha_1$ radiation and KCl (a_0 = 0.6292 nm) as an internal standard.

Specimens were prepared for high-resolution electron microscopy by crushing in an agate mortar under *n*-butanol. A drop of the resulting suspension was placed on a copper grid covered by a holey carbon film. Thin fragments which projected over holes in the film were examined using a JEM 100B electron microscope fitted with a goniometer stage. Scanning electron microscopy was carried out on a JSM 35 instrument operated at 35 kV.

Phases present in the catalysts were identified by comparison with the X-ray data given by Salje *et al.* (*16*) for the series $Mo_xW_{1-x}O_3$ and by Magnéli *et al.* (*18*) for the series $(Mo_xW_{1-x})_nO_{3n-1}$, and by electron microscopy and diffraction under the high resolution conditions described by Allpress and Sanders (*19*). This requires fragments of crystals to be oriented such that the *b* axis is parallel to the electron beam, enabling the (010) projection of the structure to be imaged. In addition selected area diffraction patterns can be taken which enable the orientation of the *CS* planes and the *n* values in the formulae above to be determined (*20*).

In addition to these structural studies a bulk analysis was carried out using flame spectrophotometry to determine the amounts of molybdenum and tungsten in the samples after synthesis. A surface analysis was also performed on the $Mo_xW_{1-x}O_3$ series using XPS, appropriate molybdenum and tungsten standards being used for calibration. Surface areas of some samples were measured by argon adsorption.

c. Catalytic evaluation. The reaction was performed by passing a mixture of propene, air, and nitrogen over 0.5 g of catalyst which was packed in a $\frac{1}{4}''$ o.d. glass-lined stainless-steel tube. The reactor tube was surrounded by a resistively heated tube furnace regulated by a temperature controller. A continuous flow of product gases was sampled automatically at intervals and analyzed by two gas chromatographs.

The gases N_2, O_2, CO, and CO_2 were analyzed by a katharometer. Initial separation took place on a Porapak T column, then N_2, O_2, and CO were directed onto a molecular sieve column and CO_2 onto a Porapak Q column by an automatic column switch mechanism. All columns were at 60° C. Propene, ethanal, and propenal were separated on a Chromosorb W column treated with β,β′-oxydipropionitrile at 45°C and analyzed by a flame ionization detector. Analysis was automated, integration of gas-chromatographic peaks being performed by a 18652A Hewlett–Packard digital integrator.

The flow rate of the feed gases, the ratio of propene to oxygen in the feed, and the reaction temperature were all carefully controlled and flow rate was standardized at 7.5 $cm^3\ min^{-1}$ to give a contact time of 3.6 sec. The series $(Mo_xW_{1-x})_nO_{3n-1}$ was tested at 500°C with a propene to oxygen ratio of 1 : 1 and 2 : 1, while the series $Mo_xW_{1-x}O_3$ was tested at 500°C and a ratio of 1 : 1.

In order to determine the effect of oxidation upon the catalytic behavior of the series $(Mo_xW_{1-x})_nO_{3n-1}$, examples were first tested under standard conditions and then oxidized *in situ* by passing oxygen over the catalyst in the reactor for 16 hr at 500°C. The standard test conditions were then reapplied. In addition some samples were oxidized by heating in a furnace in air at 750°C prior to retesting.

In the following discussion, conversion and selectivity are defined as follows:

$$\text{Conversion} = \frac{\text{Moles of propene converted to products}}{\text{Moles of propene initially present}}$$

$$\text{Propenal selectivity} = \frac{\text{Moles of propene converted to propenal}}{\text{Moles of propene converted}}$$

$$\begin{array}{l}\text{(Propenal + ethanal)}\\ \text{selectivity}\end{array} = \frac{\text{(Moles of propene converted to propenal or ethanal)}}{\text{Moles of propene converted}}$$

The number of moles of propene feed was obtained by summation of all the carbon-containing products while "moles of propene converted" was derived from this figure minus the unreacted propene. This method of analysis was adopted because it was essential very carefully to balance the feed gases to give a fixed propene to oxygen ratio, making accurate routine determination of the feed propene impractical. The absence of any other significant products, together with occasional checks on the carbon mass balance, showed this method to be reliable. Similarly, due allowance was made for oxygen in the oxygenated products in determining the initial oxygen concentration.

STRUCTURAL RESULTS

a. General

The method for preparing the specimens studied here and described above was arrived at after some difficulties were encountered in the preliminary work. Generally molten MoO_3 tended to react with the silica tubes and so in order to prevent the melting of unreacted MoO_3 gradual heating up to 700°C was adopted and high temperatures were avoided. Also when molybdenum metal was used to perform the reduction there was evidence for the production of undesired phases and irreproducible products. For example, one sample of composition $Mo_{0.9}W_{0.1}O_{2.90}$ was found to contain a tetragonal phase, probably $(Mo,W)_5O_{14}$, and MoO_3. For this reason it was decided to use MoO_2 rather than molybdenum metal.

Flakes of cristobalite were a common impurity in the samples and had to be physically separated. These resulted from the devitrification of the silica tube under the influence of the MoO_3 and WO_3 reactants, even though cristobalite is normally only stable above about 1300°C. This is a common problem in sealed ampoule work and has been commented on before (*21*).

There are also appreciable difficulties involved in phase analysis of the products, particularly when using powder X-ray diffraction. The general problems associated with the identification of *CS* structures and the need for high resolution powder cameras rather than diffractometers have been stressed in several recent publications (*22–24*). Even using high resolution techniques only very well-ordered phases can be detected. Electron diffraction patterns obtained from small regions of crystal are of value in interpreting the structures present in a sample, but even these do not present a true picture of the complexity often present in the sample. In practice the true microstructures of these phases can only be determined by high resolution transmission electron microscopy, which gives an image of a crystal even when it is severely disordered.

b. Series $Mo_xW_{1-x}O_3$

The phases identified in these samples are listed in Table 1. On the whole, the majority of these are WO_3-like structures differing from each other only in the distortions present in the MO_6 octahedra (*15*). Examination of $Mo_{0.6}W_{0.4}O_3$ with the electron microscope confirmed the presence of only WO_3-like material. Comparison of X-ray films before and after catalysis showed no important changes although there were possibly some small changes in symmetry.

The results of the bulk and surface analyses for molybdenum and tungsten are shown in Table 2. The analyzed bulk composition contains slightly less molybdenum than the "as made" bulk composition, possibly due to some evaporation of MoO_3 in the sealed tubes. There is also some evidence of surface enrichment in molybdenum.

TABLE 1

Phases Identified in the Series $Mo_xW_{1-x}O_3$ by X-Ray Diffraction

Prepared composition x	Phases present[a]
0.8	$\zeta + \theta + (\epsilon) + MoO_3$
0.7	$\zeta + \theta + (\epsilon)$ + trace MoO_3
0.6	$\zeta + \theta + (\epsilon)$
0.5	$\zeta + \theta + (\epsilon)$
0.4	$\zeta + \theta + (\epsilon)$
0.2	$\zeta + \alpha$

[a] The notation is that described by Salje *et al.* (*16*).

TABLE 2

Analytical Results for the Series $Mo_xW_{1-x}O_3$

Prepared composition x	Bulk chemical analysis x	XPS surface composition x
0.8	0.69	0.75
0.7	0.62	0.65
0.6	0.58	0.60
0.5	0.46	Not analyzed
0.4	0.37	0.51
0.2	0.19	Not analyzed

c. Series $(Mo_xW_{1-x})_nO_{3n-1}$

All samples before catalysis were *CS* structures with no free MoO_3. An estimate could be made of the value of *n* from X-ray data, although as *n* increased the amount of disorder increased and it became harder to be precise as to its value. Observation of fragments in the electron microscope also gave values of *n* which were generally in fair agreement with the X-ray results. Table 3 summarizes these results. Figure 3 shows diffraction patterns of two fragments, one from an ordered crystal of the $(Mo,W)_{10}O_{29}$ type, and one which contains disordered $(W,Mo)_{10}O_{29}$ and $(W,Mo)_{12}O_{34}$. The results

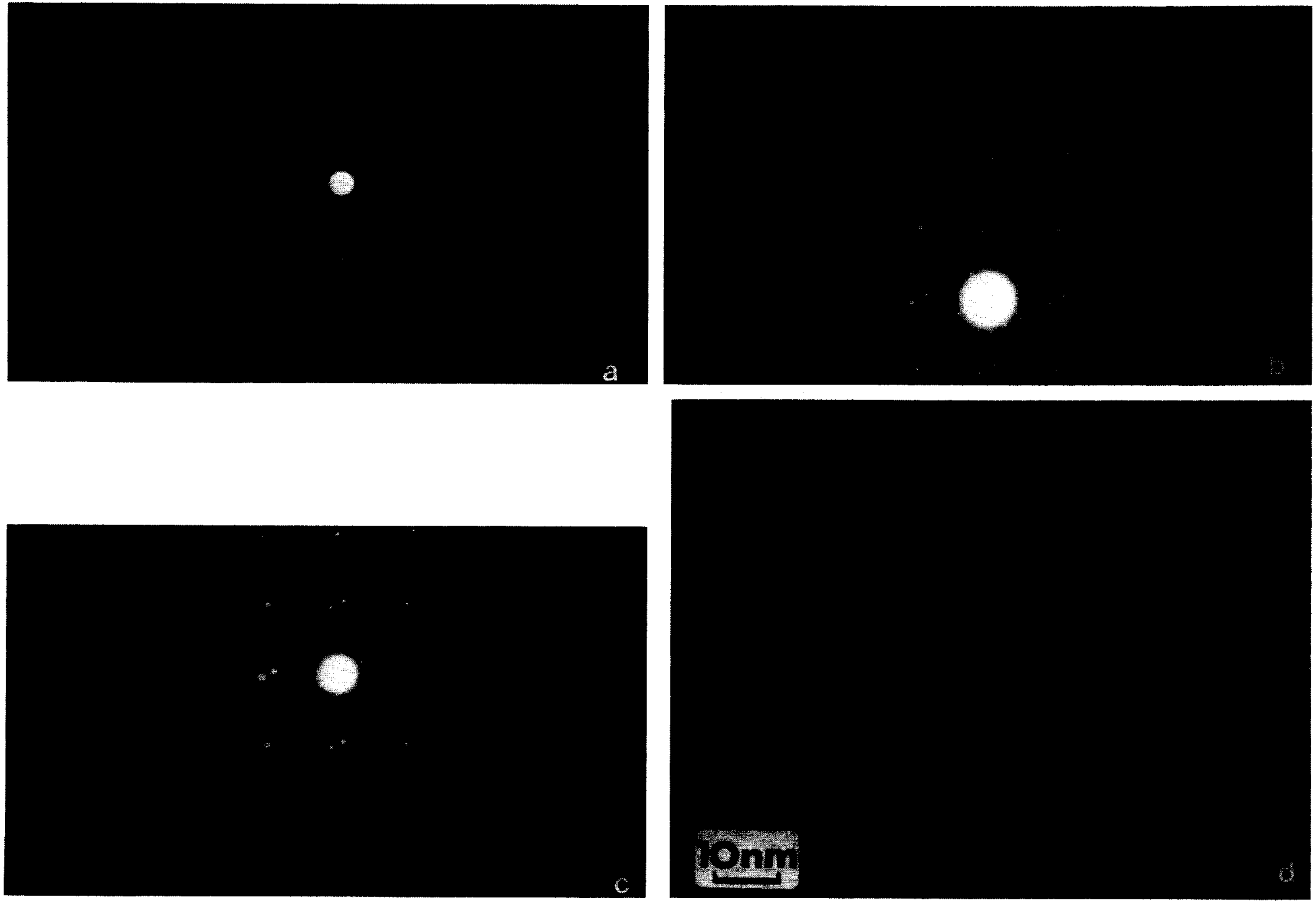

FIG. 3. (a–c) Electron diffraction patterns from (a) $Mo_{0.5}W_{0.5}O_3$, (b) a crystal fragment containing ordered {102} *CS* planes with $n = 10$, and (c) a crystal fragment containing disordered {102} *CS* planes, $n = 10$ and 12. (d) Micrograph of a crystal fragment containing {102} *CS* planes.

TABLE 3

X-Ray and Electron Microscopic Analysis of the *CS* Plane Structure of the Reduced Series $(Mo_xW_{1-x})_nO_{3n-1}$

Prepared composition	Value of *n* estimated from X-ray data (*18*)	Value of *n* derived from high resolution microscopy[a]
$MoO_{2.875}$	8	8 (1)[a]
$Mo_{0.9}W_{0.1}O_{2.90}$	9	9 (3); 8 (1); 10 (1)
$Mo_{0.8}W_{0.2}O_{2.90}$	10	10 (4); 10 and 12 (1)
$Mo_{0.7}W_{0.3}O_{2.917}$	12	12 (3); 11 or 12 (1)
$Mo_{0.6}W_{0.4}O_{2.917}$	12 or 14	12 (3); 14 (2)
$Mo_{0.5}W_{0.5}O_{2.929}$	14	14 (2); 12 and 14 (1) 12 (1); 14 or 15 (1)
$Mo_{0.4}W_{0.6}O_{2.95}$	14	14 (2); 14 or 15 (1) 15 or 16 (1)

[a] Parentheses denote the number of crystal fragments of each type found.

of flame spectrophotometric analysis for the bulk metals content are given in Table 4.

Comparison of X-ray films before and after catalysis showed that the samples were generally stable to the reaction conditions. One or two samples did undergo oxidation to some extent to give small amounts of the ζ phase of $Mo_xW_{1-x}O_3$ and MoO_3 and this was accompanied by a color change from black to grey/green. Examination of samples in the electron microscope did not reveal any increase in the disorder of the *CS* phases or any change in the value of *n* as a result of catalytic reaction. An exception was the sample $MoO_{2.875}$ which was found to oxidize rapidly to MoO_3 under reaction conditions.

d. *Series* $(Mo_xW_{1-x})_nO_{3n-1}$ *after Oxidation*

Scanning electron microscopy showed no change in the crystal morphology as a result of overnight oxidation at 500°C. X-Ray diffraction gave patterns typical of the series $Mo_xW_{1-x}O_3$ while transmission microscopy confirmed that the majority of crystal fragments were WO_3-like in structure without *CS* planes being present. The occasional crystal fragment was however found to be unchanged, that is to say it was a *CS* phase similar to the original material. It is not clear whether such fragments were present as a result of incomplete oxidation or some other effect. Partial removal of *CS* planes (i.e., a reduction in the value of *n*) was not observed. The surface area of the sample $Mo_{0.8}W_{0.2}O_{2.90}$ was found to increase from 1.3 to 4.9 m²/g as a result of the *in situ* oxidation treatment. Prolonged oxidation in air at 750°C gave similar X-ray diffraction patterns to the fully oxidized $Mo_xW_{1-x}O_3$ materials, but the crystals were found to have agglomerated to give well rounded edges and corners. Their habit was therefore quite different to the reduced samples.

TABLE 4

Chemical Analysis of Series $(Mo_xW_{1-x})_nO_{3n-1}$

Prepared composition value of *x*	Chemical analysis Values of *x*
0.9	0.86
0.8	0.76
0.7	0.66
0.6	0.57
0.5	0.43
0.4	0.34

CATALYTIC RESULTS

a. *Series* $(Mo_xW_{1-x})O_{3n-1}$

In general the catalytic behavior of these materials showed little change under constant reaction conditions during the course of the experiment. Conversion was low for all samples and there was no trend across the series of compositions.

Selectivity was found to be sensitive to the ratio of propene to oxygen in the feed and this ratio was therefore carefully controlled in order not to obscure small differences between catalysts. This effect is illustrated in Fig. 4. The influence of reaction temperature at a constant propene to oxygen ratio of 1 : 1 is shown in Fig. 5.

The catalytic behavior at two fixed compositions is summarized in Fig. 6 where it may be seen that there is a decrease in selectivity as the concentration of tungsten increases and the density of *CS* planes decreases.

b. Series $Mo_xW_{1-x}O_3$

The catalytic behavior of these materials did not change during reaction. This stability is in agreement with the structural observations. Conversion was again low for all samples and no significant trend could be established as a function of composition. A comparison of the conversion/selectivity data with that for the reduced series is given in Fig. 7.

The important features to note are:

(i) reduced samples show a higher conversion per pass and selectivity than oxidized samples with the same amounts of molybdenum and tungsten. (Since the surface areas of both oxidized and reduced samples were very similar, approximately 1 m^2/g, this indicates a higher specific conversion rate with the reduced series of catalysts);

(ii) in the oxidized series, an increase in selectivity on moving away from MoO_3 toward the tungsten-containing phases is followed by a decrease as the concentration of tungsten increases across the series. This gives rise to a maximum in selectivity at about $x = 0.6$ and it would appear therefore that, in these oxides, the highest selectivities are found when molybdenum atoms are situated in the open WO_3-like lattice.

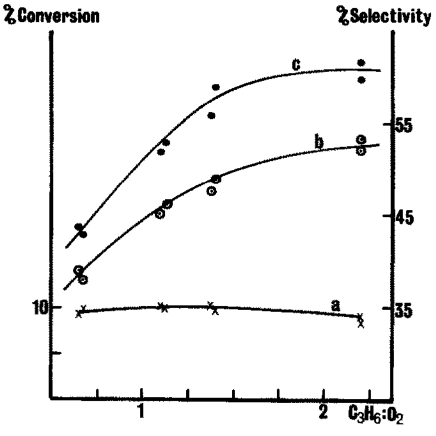

FIG. 4. Effect of propene to oxygen ratio on (a) conversion per pass, (b) propenal selectivity, and (c) propenal and ethanal selectivity for the oxidation of propene at 500°C over $Mo_{0.7}W_{0.3}O_{2.917}$.

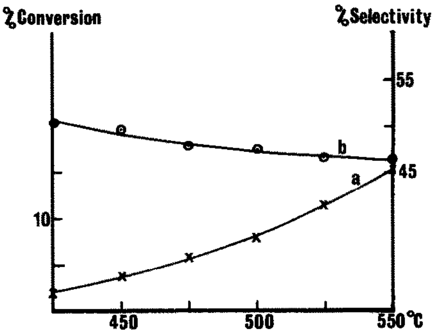

FIG. 5. The effect of temperature on propene oxidation; (a) conversion per pass, (b) selectivity to propenal over $Mo_{0.5}W_{0.5}O_{2.929}$.

c. Series $(Mo_xW_{1-x})_nO_{3n-1}$ *after Oxidation*

Heating the members of series $(Mo_xW_{1-x})_nO_{3n-1}$ in air in the absence of hydrocarbon produced changes in the catalytic performance dependent upon temperature and the heating period. An overnight oxidation at 500°C reduced the conversion per pass to a level typical of the series $Mo_xW_{1-x}O_3$ even though the surface area increased from 1.3 to 4.1 m^2/g as a result. The selectivity, however, remained little changed. Prolonged oxidation at 750°C gave a similar reduction in conversion per pass but caused selectivity to fall, approaching values typical of the series $Mo_xW_{1-x}O_3$ (Table 5).

TABLE 5

The Effect of Oxidation Conditions on the Catalytic Performance of Members of the Reduced Series $(Mo_xW_{1-x})_nO_{3n-1}$ after Oxidation

	$Mo_{0.4}W_{0.6}O_{2.95}$		$Mo_{0.8}W_{0.2}O_{2.90}$		$Mo_{0.5}W_{0.5}O_{2.929}$		
	Before oxidation	After short-term oxidation at 500°C	Before oxidation	After short-term oxidation at 500°C	Before oxidation	After short-term oxidation at 500°C	After long-term oxidation at 750°C
% Conversion	11.0	6.7	5.0	3.1	11.2	6.3	5.5
% Propenal selectivity	49.9	52.2	56.3	61.3	46.6	44.4	35.2
% (Propenal + ethanal) selectivity	49.9	52.2	59.8	61.3	49.2	44.4	35.2

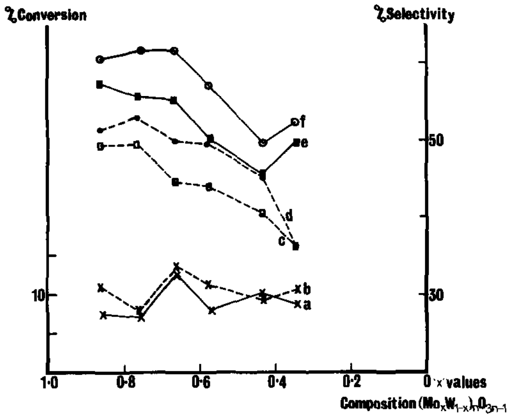

FIG. 6. The variation of conversion and selectivity with molybdenum concentration x for the series $(Mo_xW_{1-x})_nO_{3n-1}$ at two different propene to oxygen molar ratios at constant temperature (500°C). (a) Conversion, $C_3H_6:O_2 = 2:1$, (b) conversion, $C_3H_6:O_2 = 1:1$, (c) propenal selectivity, $C_3H_6:O_2 = 1:1$, (d) (propenal + ethanal) selectivity, $C_3H_6:O_2 = 1:1$, (e) propenal selectivity $C_3H_6:O_2 = 2:1$, and (f) propenal + ethanal) selectivity, $C_3H_6:O_2 = 2:1$.

d. The Pure Oxides

The catalytic performance of pure WO_3 was found to depend markedly upon the heat treatments to which it had been subjected.

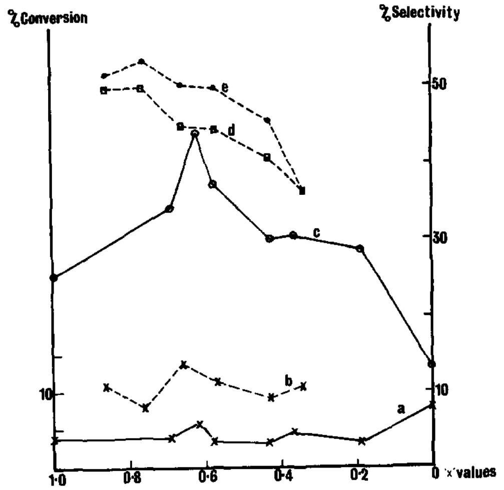

FIG. 7. Catalytic behavior as a function of catalytic composition for the series $Mo_xW_{1-x}O_3$ [(a) conversion, (c) propenal selectivity] and $(Mo_xW_{1-x})_nO_{3n-1}$ [(b) conversion, (d) propenal selectivity, (e) propenal and ethanal selectivity] for reaction at 500°C and propene to oxygen ratio 1 : 1.

Commercial WO_3 gave high conversions per pass but low selectivity. Calcining at increasing temperatures resulted in recrystallization and an accompanying decrease in conversion rate only above 700°C. Surprisingly, heating at 775°C in a vacuum for 11 days gave a green material which was very selective, whereas the same treatment in air gave a yellow material which was very unselective under the same reaction conditions. The catalytic performance of MoO_3 was not significantly altered by its method of preparation. The oxide $MoO_{2.875}$ initially gave much higher selectivity than MoO_3 but oxidation to MoO_3 occurred rapidly and the selectivity was reduced accordingly.

DISCUSSION

The results presented above lead to a number of definite conclusions about the role of the underlying structure in the catalytic reaction that we have studied. When we consider the fully oxidized $Mo_xW_{1-x}O_3$ materials we note a marked increase in selectivity on passing from MoO_3 to the compounds with some tungsten present. The phase diagram given by Salje *et al.* (*16*) suggests a change in structural type when $x = 0.95$ from the MoO_3 structure to the more open WO_3-like structure. The observed increase in selectivity is probably associated with this change. Our graphs do not show a step-like increase, but this is not surprising because the $Mo_{0.8}W_{0.2}O_3$ sample contains some free MoO_3 which would be expected to lower the overall selectivity.

We also note that the selectivity then decreases as we increase the tungsten content toward the value found for WO_3 (*6*). This result, together with that just mentioned, suggests that the major catalytic role in the reaction is taken by molybdenum, with tungsten acting as a less active diluent. However, the MoO_3 structure itself is not so suitable for the reaction as the open WO_3-like structure, and the initial addition of a small percentage of WO_3 to the MoO_3 parent therefore has a very favorable impact upon the reaction.

When the results from the reduced oxides are examined, several differences in behavior from the fully oxidized materials are apparent. Significantly higher selectivity confirms that *CS* planes are intimately involved in the catalytic reaction. The observed decrease in selectivity across the range of compositions can in part be attributed to increasing tungsten content, as already noted for the fully oxidized materials. Decreasing *CS* plane density is however a concurrent effect. These two factors will affect a number of physical and chemical properties which will be discussed further below, after considering the catalytic reaction in more detail.

There is a wide agreement about the mechanism of the oxidation of propene to propenal over mixed metal oxide catalysts. The first step is the adsorption of the propene molecule onto the catalyst surface followed by the abstraction of a hydrogen atom to form an allyl radical. A second hydrogen abstraction and the addition of an oxygen atom from the lattice then occurs, followed by desorption of the propenal molecule. The role of gaseous oxygen is to reoxidize the lattice. The mechanism for complete oxidation is rather less well established. Complete oxidation to CO or CO_2 may occur through further oxidation of propenal or through oxidation of propene by a parallel route, employing either lattice oxygen (*25*) or surface adsorbed activated oxygen (*4*).

The ideas we wish to explore are that *CS* planes may play a role in the transport of oxygen within the lattice under catalytic reaction conditions and in the actual insertion of oxygen into the propene molecule at the catalytic site by alteration of the linkage of metal–oxygen polyhedra. However, the introduction of *CS* planes into the WO_3-like lattice is necessarily accompanied by several other factors which should be considered: (a) the catalyst is in a reduced state and the electron and oxygen mobilities will be altered, (b) new adsorption sites may have been introduced, e.g., within rectangular tunnels and at the intersection of *CS* planes with the surface, (c) variation of the density of *CS* planes by altering the molybdenum to tungsten ratio also alters the cationic distribution at the surface, and (d) molybdenum is unlikely to be randomly distributed throughout the lattice but may actually be concentrated in the *CS* planes (*26*).

A clear conclusion from our results is that the presence of *CS* planes in the catalysts is associated with a higher conversion. This may be seen by contrasting the performance of the reduced series both with its own performance after oxidation (which has been shown at least to reduce the number of shear planes if indeed it does not entirely eliminate them) and with that of the oxidized series. These observations are thus consistent with an increased rate of oxygen transport in the presence of *CS* planes resulting in a more rapid regeneration of surface sites.

Interpretation of the selectivity results is less straightforward. Increasing tungsten content is of itself sufficient to explain the fall in selectivity with the decrease in the density of the *CS* planes across the series, since the rate of decrease is comparable with that of the oxidized series. Although we cannot link high *CS* plane density with high selectivity from this trend, the fact that members of the reduced series of catalysts were more selective than corresponding members of the oxidized series does suggest that the presence of *CS* planes increases selectivity.

Further conclusions may be drawn by considering the effect on selectivity of the temperature at which the *CS* planes were oxidized. Oxidation at 500°C was effective in removing the majority of the *CS* planes and regenerating the basic WO_3-like lattice. The selectivity was, however, little altered, indicating that the electronic factor in the reduced materials is relatively unimportant. Only when the oxidation temperature was raised to 750°C for prolonged periods was the catalytic behavior of the fully oxidized $Mo_xW_{1-x}O_3$ series duplicated. The most likely reason for these variations lies in the molybdenum distribution. It would seem reasonable to suppose, following the study by Viswanathan and Salje (*26*), that molybdenum atoms are preferentially located in the *CS* planes. If this is the case it would suggest that while a temperature of 500°C is effective in introducing oxygen into the rectangular tunnels between the blocks of four edge-sharing octahedra in the *CS* planes, higher temperatures are required to redistribute molybdenum throughout the lattice. We are therefore led to the conclusion that not only is the molybdenum taking the major role catalytically in these materials, but that its particular association or clustering within the *CS* planes, that is the Mo–Mo geometry, is also important. It is possible that such a configuration is therefore a useful template in the reaction studied.

In conclusion we can say that our experiments have proved beyond doubt that *CS* planes can have a significant effect on a catalytic reaction, a result not conclusively demonstrated in the past. However, we also note that the most important factor may be the segregation of particular chemical species within the *CS* planes rather than other attributes of the structure. This leads us to a number of future developments. Clearly, if our ideas are correct, then other molybdenum compounds with similar geometry should show similar catalytic behavior, while compounds with different geometries will show different behavior. In particular we plan to study other types of *CS* structure in the reduced molybdenum oxides, and the oxides which contain, not *CS* planes, but pentagonal columns of molybdenum atoms as a structural motif, to see how these relate to the materials already investigated.

As far as the present study is concerned, there are still some points to be clarified. First, the structural behavior of the $(Mo_xW_{1-x})_nO_{3n-1}$ phases on oxidation needs to be examined in detail. This project is at present underway and the results will be reported in a future communication. Second, more microstructural information on the nature of these materials would be desirable. In particular, if we could obtain analytical data from the inter-*CS* plane volumes of these phases, to determine Mo distributions, this would be of immense interest. Advances in analytical electron microscopy suggest that this difficult problem may be amenable to solution within the next few years. Finally, we should mention that our study has largely attempted to correlate bulk structures with catalytic behavior. Nevertheless, the catalytic reaction is a surface process. More information on the surface structures of such materials is badly needed. Once again, advances in electron microscopy afford hope that this information will become available in the near future.

ACKNOWLEDGMENTS

The authors are indebted to I.C.I. PLC for the provision of facilities and permission to publish and to H. Herniman for practical assistance.

REFERENCES

1. O'Keeffe, M., "Fast Ion Transport in Solids," p. 233. North Holland, Amsterdam, 1973.
2. Stone, F. S., NATO Advanced Study Inst. "Fundamental Principles in Heterogeneous Catalysis" (Venice 1971), XIII-31 (1971).
3. Stone, F. S., *J. Solid State Chem.* **12,** 271 (1975).
4. Haber, J., "The Chemistry and Uses of Molybdenum," Proc. 3rd Int. Conf. Molybdenum p. 119. Climax Molybdenum Co., 1979.
5. Schiavello, M., Tilley, R. J. D., De Rossi, S., and Iguchi, E., *Z. Phys. Chem. N.F.* **104,** 165 (1977).
6. De Rossi, S., Iguchi, E., Schiavello, M., and Tilley, R. J. D., *Z. Phys. Chem. N.F.* **103,** 193 (1976).
7. Schiavello, M., Pepe, F., Cannizzaro, M., De Rossi, S., and Tilley, R. J. D., *Z. Phys. Chem. N.F.* **106,** 45 (1977).
8. De Rossi, S., Iguchi, E., Schiavello, M., and Tilley, R. J. D., *React. Kinet. Catal. Lett.* **6,** 201 (1977).
9. Schiavello, M., *Chim. Ind. (Milan),* **61,** 554 (1979).
10. De Rossi, S., Iguchi, E., Schiavello, M., and Tilley, R. J. D., *J. Catal.* **61,** 256 (1980).
11. Gai, P. L., *Phil. Mag.* **43,** 841 (1981).
12. Kihlborg, L., *Arkiv. Kemi* **21,** 471 (1963).
13. Ekström, T., *Chem. Comm. Univ. Stockholm* **7** (1975).
14. Ekström, T., and Tilley, R. J. D., *Chem. Scripta* **16,** 1 (1980).
15. Tilley, R. J. D., *Chem. Scripta* **14,** 147 (1978).
16. Salje, E., Gehlig, R., and Viswanathan, K., *J. Solid State Chem.* **25,** 239 (1978).
17. Ekström, T., Salje, E., and Tilley, R. J. D., *J. Solid State Chem.* **40,** 75, (1981).
18. Magnéli, A., Blomberg-Hanson, B., Kihlborg, L., and Sundkvist, G., *Acta Chem. Scand.* **9,** 1382 (1955).
19. Allpress, J. G., and Sanders, J. V., *J. Appl. Crystallogr.* **6,** 165 (1973).
20. Bursill, L. A., and Hyde, B. G., *J. Solid State Chem.* **4,** 430 (1972).
21. Ekström, T., and Tilley, R. J. D., *J. Crystallogr. Growth* **38,** 197 (1977).
22. Booth, J., Ekström, T., Iguchi, I., and Tilley, R. J. D., *J. Solid State Chem.* **41,** 293, (1982).
23. England, P., Booth, J., Ekström, T., and Tilley, R. J. D., *J. Solid State Chem.* **44,** 60 (1982).
24. Sundberg, M., Ekström, T., and Tilley, R. J. D., in preparation.
25. Keulks, G. W., and Krenzke, L., Proc. Int. Congr. Catalysis, 6th (London 1976), p. 806. Chemical Society, London, 1977.
26. Viswanathan, K., and Salje, E., *J. Solid State Chem.,* in press.